Modeling of microwave discharges in the presence of plasma resonances

Yu. M. Aliev and A. V. Maximov
Lebedev Institute, Russian Academy of Sciences, 117924 Moscow, Russia

U. Kortshagen and H. Schlüter
Institut für Experimentalphysik II, Ruhr-Universität, 44780 Bochum, Germany

A. Shivarova
Faculty of Physics, Sofia University, 1126 Sofia, Bulgaria
(Received 13 June 1994; revised manuscript received 28 October 1994)

This study presents a kinetic model of microwave generated discharges sustained, under the conditions of a diffusion controlled regime, by the propagation of azimuthally symmetric surface waves. The effect of the plasma resonances, which can appear over the radial density profile in the vicinity of the walls and lead to sharp peaks in the radial component of the high-frequency wave electric field in the plasma, is introduced. This effect modifies the surface wave damping and results in a collisional as well as collisionless (quasilinear) transfer of energy from the radial field component to the plasma. In the Boltzmann equation the latter appears as a third channel of energy transfer, which is added to the Joule heating by the axial and radial wave field components. The spatially inhomogeneous Boltzmann equation for the electron-energy distribution function, which accounts for the radial ambipolar field, is solved in the nonlocal approximation. A complete set of relations is formed by simultaneous consideration of the fluid equations for the ion motion and the field equations for the surface wave electric field. The problem is solved numerically. It yields self-consistent radial electron density profiles and radial electric field distributions. The obtained solutions evidence indeed the occurrence of plasma resonances. The study is extended also to obtaining results for the axial variation of the (radially averaged) electron density. It turns out that the widely used concept of approximate constancy of wave power absorbed by one electron in a diffusion controlled regime keeps its validity also in the presence of plasma resonances and of the corresponding collisional, as well as collisionless, power transfer to the plasma in the resonance regions.

PACS number(s): 52.80.Pi, 51.10.+y

I. INTRODUCTION

The surface wave (SW) sustained plasmas, developed as a new branch of the microwave generated discharges, have attracted steadily increasing interest [1,2] over the 20 years of their study. This type of discharges exhibits overdense plasmas: The spatially averaged plasma frequency $\overline{\omega_p}$ is larger than the wave frequency ω and this ensures the condition for SW propagation. However, due to a spatial (radial) plasma density inhomogeneity, local plasma resonances [3] $\omega_p(r = r_s) = \omega$ can occur over the radial density profile close to the discharge walls. These resonances can result in large and sharp peaks of the radial component of the SW electric field and can affect the wave damping [3–5].

The kinetic modeling of the discharges sustained by SW propagation developed for the conditions of a diffusion controlled regime has usually followed methods common for describing the discharge maintenance by high-frequency fields in general, namely, in accounting for the collisional Joule heating by the wave field [6–12]. The modeling has been based on local and nonlocal approaches, i.e., without and with accounting for the radial plasma inhomogeneity and for the stationary ambipolar field, which may be larger than the effective high-frequency field maintaining the discharges (see, e.g., the estimations in [13]). On the basis of these studies, the concept of a constant average absorbed power per electron Θ [10] (along the discharge length) has emerged as a good approximation. It has been widely used as an empirical assumption in studies on the axial structure of the discharges on the basis of fluid plasma models [14–17]. (In the fluid models, a constant value of the electron temperature [16,18] taken as measure of the mean electron energy is a concept equivalent to $\Theta = \text{const.}$)

Recently [19–21] attention has been paid to the existence of plasma resonance regions over the radial density profile. The enhanced radial electric field there can influence the energy balance and, therefore, should be taken into account in the discharge modeling. The role of this effect on the radial temperature distributions [21], obtained in the framework of the fluid plasma model, has recently been extended to establishing its effect on the axial density profile [22–24]. In the kinetic modeling of the discharges, the idea for the role of the plasma resonance regions has been treated up to now only analytically [19,20]. It has been shown that this effect results in fast electron generation [19] and, in general, in the

appearance of a new channel of power transfer from the wave to the plasma [20]. This mechanism is collisionless and stems from the quasilinear distortion of the electron velocity distribution function: an effect discussed in the quasilinear theory and the theory of weak plasma turbulence [25]. It can be interpreted as a Cherenkov effect of wave-particle interactions. Since the relative efficiency of the different heating processes may vary strongly in different regimes of SW discharges, it is important to account for all the channels of energy transfer contributing to the formation of the electron distribution function in the velocity space.

In the numerical model presented below the collisionless energy transfer is included in the inhomogeneous Boltzmann equation as a third channel in addition to the (traditional) two channels from the collisional Joule heating via the axial and the radial field component. A fully self-consistent formulation is achieved by simultaneous consideration of a set of fluid equations for the ion motion and the SW electric field equations. Thus, in contrast to previous investigations where it was necessary to postulate the existence of the plasma resonance [4,19–21], the resonance of the radial field component turns out to be a result of the fully self-consistent model in the present study. It is the aim of this paper to investigate the influence of the plasma resonance on the SW discharge on the basis of this self-consistent concept. Mainly two aspects will be addressed: the importance of the collisionless heating mechanism, which is connected to the appearance of the resonance, and the influence of the resonance on the axial structure of the discharge.

The paper is organized as follows. In Sec. II the formulation of the kinetic model is described. At first a short sketch of the derivation of the term on diffusion in velocity space, which yields collisionless heating by the resonant electric field and has to be included in the kinetic formulation, is presented. Afterwards the solution of the spatially inhomogeneous Boltzmann equation within the nonlocal approximation is discussed. The equations necessary to set up a complete, self-contained set of equations are given in the final part of Sec. II. In Sec. III the two main aspects of the resonant interactions are investigated: namely, their influence on the mechanism of power transfer from the wave to the plasma and their influence on the formation of the axial electron density profile of the discharge. The presented numerical results are discussed, and basic features are commented on and compared to previous analytical studies. A summary of the main conclusions and an outlook to forthcoming work is given in Sec. IV.

II. DESCRIPTION OF THE MODEL

The discharge is sustained by a propagating surface wave with frequency ω and field components $\mathcal{E}_r$, $\mathcal{H}_\varphi$, $\mathcal{E}_z \neq 0$. The waveguide configuration consists of a plasma cylinder with radius a, surrounded by a glass tube with radius b and permittivity ε_g, and vacuum.

The description of the electron kinetics is based on the Boltzmann equation

$$\frac{\partial \mathcal{F}}{\partial t} + \vec{v}\cdot\vec{\nabla}_r\mathcal{F} - \frac{e}{m}\vec{\mathcal{E}}\cdot\vec{\nabla}_v\mathcal{F} = \left(\frac{\partial \mathcal{F}}{\partial t}\right)_{\text{coll}}, \tag{1}$$

where $\mathcal{F} \equiv \mathcal{F}(\vec{r},\vec{v},t)$ is the electron velocity distribution function, $\vec{\mathcal{E}}(\vec{r},t)$ is the wave electric field, and $-e$ and m are the electron charge and mass. The right-hand side of the equation represents the collisional integral.

For solving (1) with accounting for the different heating mechanisms, in particular the diffusion in the velocity space due to the quasilinear collisionless effects [20], and the inhomogeneity in the configuration space [11] due to the steady-state ambipolar field, the steps given in the subsections below have been taken.

A. Collisionless energy transfer

The procedure for obtaining the contribution of the collisionless energy transfer from the high-frequency wave field to the plasma is based on the theory of weak plasma turbulence [25]. Its applicability to the case of SW sustained discharges is given in detail in [20]. This channel of energy transfer stems from the plasmon-particle interactions. Plasmons are generated as collective oscillations in the region around the resonance point $r = r_s$ on the radial density profile, where the plasma frequency equals the wave frequency [$\omega_p(r = r_s) = \omega$]. At the resonant point the real part of the plasma permittivity $\varepsilon_p(r)$ becomes zero. The continuity of the normal component of the dielectric displacement yields a sharp, resonant enhancement of the radial electric field component in this region. The averaged quadratic effect of the fast varying parts of the field and of the distribution of the particles, which are in resonance with the field — an averaged effect of phase mixing — results in changes of the slowly varying part of the distribution of the "resonance" particles. The final result is a diffusionlike term in the equation for the distribution function which acts in the velocity range of the "resonance" particles.

The quasilinear term for diffusion in velocity space is in principle obtained as follows (for a more detailed presentation the reader is referred to Refs. [19,20]).

(1) The long and short scale variations (with respect to the electron mean free path λ_e) of both the electric field $\mathcal{E}(\vec{r},t)$ and the distribution function $\mathcal{F}(\vec{r},\vec{v},t)$ are separated and presented in the following form:

$$\begin{aligned}\vec{\mathcal{E}}(\vec{r},t) &= \langle\vec{E}(\vec{r},t)\rangle + \vec{e}(\vec{r},t),\\ \mathcal{F}(\vec{r},\vec{v},t) &= \langle F(\vec{r},\vec{v},t)\rangle + f(\vec{r},\vec{v},t)\,.\end{aligned} \tag{2}$$

The first terms on the right-hand side are the slowly varying parts, which have been averaged over the short scale variations. The second terms are the microfield and the short scale contributions to the distribution function on the λ_e scale, respectively.

(2) The slow (i.e., averaged over the SW period $2\pi/\omega$) and fast time variations are separated:

$$\langle \vec{E}(\vec{r},t)\rangle = \vec{E}(\vec{r},t) + \vec{\tilde{E}}(\vec{r},t),$$
$$\langle F(\vec{r},\vec{v},t)\rangle = F(\vec{r},\vec{v},t) + \tilde{F}(\vec{r},\vec{v},t)\,. \tag{3}$$

Here the first terms on the right-hand side denote the time averaged quantities. It is also assumed that the time averaged microfield $\vec{e}$ is zero. This excludes considerations of collisionless double layers.

(3) The set of equations obtained from the Boltzmann equation (1) after making substitutions (2) and (3) yields the quasilinear term from small scale averaging and time averaging (denoted here by the overbar):

$$S_{\rm ql}(F) = \frac{e}{m}\overline{\left\langle \vec{\tilde{e}}\cdot\frac{\partial\tilde{f}}{\partial\vec{v}}\right\rangle}\,. \tag{4}$$

This term stems from the short scale quantities, but it affects the slowly varying part $F(\vec{r},\vec{v},t)$ of the distribution function. It should be added to the collisional integral in the right-hand part of Eq. (1) for the slowly varying part of the distribution function $F(\vec{r},\vec{v},t)$. In fact, since the nature of the quasilinear effect is a diffusion in the velocity space, expression (4) can be evaluated and presented in the form (see [19])

$$S_{\rm ql}(F) = \frac{\partial}{\partial\vec{v}}\left[\mathsf{D}_{\rm ql}(\vec{v},\vec{r},t)\frac{\partial F}{\partial\vec{v}}\right]\,. \tag{5}$$

For calculating $\mathsf{D}_{\rm ql}(\vec{v},\vec{r},t)$, the quasilinear diffusion tensor due to this effect, the resonantly enhanced radial electric field component associated with plasma resonances has to be introduced in a form as given in [19]. Specular reflection near the discharge walls is the boundary condition used for the resonant electrons [19,20]. This quasilinear heating term tends to favor the appearance of higher energy electrons [19].

After the introduction of the quasilinear heating term, the ordinary procedure [26,27] for solving the Boltzmann equation in series expansion in spherical harmonics in the limits of the Lorentz approximation

$$F(\vec{r},\vec{v},t) = F_0(\vec{r},\vec{v},t) + \frac{\vec{v}}{v}\cdot\vec{F}_1(\vec{r},\vec{v},t) \tag{6}$$

is applied. The case of sufficiently high frequency ω of the applied field is considered:

$$\omega > \nu_e = \varkappa\nu_m + \sum_k \nu_k\,. \tag{7}$$

Here ν_e is the energy relaxation frequency, ν_m the momentum transfer collision frequency, ν_k is that of the kth inelastic process with threshold energy u_k, $\varkappa = 2m/M_a$ is the portion of energy transferred at one electron-atom collision, and M_a is the atom mass. In cylindrical geometry and with $u = \frac{1}{2}mv^2/e$, the electron kinetic energy in voltage units, the equation for the isotropic part F_0 of the electron-energy distribution function (EEDF) becomes [26]

$$\frac{2}{3}\frac{e}{m}\left\{\frac{u^{\frac{3}{2}}}{\nu_m}\left[\vec{\nabla}_{\vec{r}}^{\,2}F_0 - \vec{\nabla}_{\vec{r}}\cdot\left(\vec{E}_s\frac{\partial F_0}{\partial u}\right)\right] + \frac{\partial}{\partial u}\left[\frac{u^{\frac{3}{2}}}{\nu_m}\left(-\vec{E}_s\cdot\vec{\nabla}_{\vec{r}}\right)F_0 + \frac{u^{\frac{3}{2}}}{\nu_m}\left(|E_s|^2 + E_{\rm eff}^2\right)\frac{\partial F_0}{\partial u}\right]\right\} + S_{\rm ql} + \frac{\partial}{\partial u}\left[u^{\frac{3}{2}}\varkappa\nu_m F_0\right]$$
$$= \sum_k\left[\nu_k(u)\sqrt{u}F_0(u) - \nu_k(u+u_k)\sqrt{u+u_k}F_0(u+u_k)\right] + S_{ee}\,. \tag{8}$$

$\vec{E}_s$ is the radial dc space charge electric field, and

$$E_{\rm eff} = \frac{1}{\sqrt{2}}\frac{\nu_m}{\sqrt{\omega^2+\nu_m^2}}\sqrt{|E_z|^2 + |E_r|^2} \tag{9}$$

is the effective field sustaining the discharge. S_{ee} denotes the electron-electron collision integral in the usual form (e.g., [26]).

The term in Eq. (8) which includes $E_{\rm eff}$ accounts for the collisional Joule heating associated with the E_z and E_r field components.

Written in the energy scale (according to the analysis in [19,20]), the quasilinear term takes the form

$$S_{\rm ql} = \frac{\partial}{\partial u}\left[D_{\rm ql}\frac{\partial F_0}{\partial u}\right]M_{\rm res}(r), \tag{10}$$

with the diffusion coefficient for the collisionless (quasilinear) energy transfer

$$D_{\rm ql} = \frac{\pi e}{2m_e}\frac{u^{\frac{3}{2}}}{\omega}|E_r(r)|^2\,\mathcal{D}(s)\,. \tag{11}$$

The function $\mathcal{D}(s)$ is defined as

$$\mathcal{D}(s) = \frac{s}{2}\left[(1-s)\exp(-s) + s^2\int_s^\infty\frac{\exp(-t)}{t}\,dt\right]$$
$$\approx \frac{s}{2}\exp(-s). \tag{12}$$

The argument s is given by

$$s = \left(\frac{2m_e\omega^2\Delta^2}{eu}\right)^{\frac{1}{2}} = 4\pi\frac{\tau}{T}\,. \tag{13}$$

Here Δ is the resonance half-width

$$\Delta = L\left(\frac{\nu_{\rm eff}}{\omega}\right)\,, \tag{14}$$

with L being the density scale length at the resonance point

$$L = \frac{1}{\left|\frac{d\ln n_e}{dr}\right|_{r=r_s}}\,. \tag{15}$$

ν_{eff} is an effective damping frequency, which describes the resonance width of the field peaks and takes into account the energy drain by collisionless heating. It is commented on below when the additional completing equations are discussed.

Computationally Δ is determined directly from the half-width of $|E_r|^2$ peaks in the resonance case and the width of the sharp increase of the field intensity towards the wall in the nonresonant case. The function M_{res} in Eq. (10) is defined as a step function:

$$M_{\text{res}}(r) = M\left(\frac{|E_r(r)|}{0.2|E_{r_{\max}}|} - 1\right), \tag{16}$$

where $M(x) = 0$ for $x \leq 0$ and $M(x) = 1$ for $x > 0$, x being the argument shown on the right-hand side of (16). This function limits the influence of the collisionless heating term to the vicinity of the resonance region.

In relation (13), $\tau = \Delta/v$ is the transit time for a single pass through the resonance and $T = (\omega/2\pi)^{-1}$ is the period of the wave. The function $\mathcal{D}(s)$ reaches its maximum for $s = 1$, i.e., for $\tau = T/4\pi$. The energy gain is thus particularly high if the transit time is short compared to the field period. It is illustrative to insert Eqs. (12) and (13) into Eq. (11). By introducing the collision frequency $\nu_c = 1/\tau_c$ one obtains

$$D_{\text{ql}} = \left(\frac{\pi e}{2m_e}\frac{u^{\frac{3}{2}}}{\nu_c}|E_r(r)|^2\right)\frac{\tau}{\tau_c}\exp\left(-4\pi\frac{\tau}{T}\right). \tag{17}$$

The first factor in the large parentheses is in a form (almost) identical to that of the (velocity space) diffusion coefficient for Joule heating in the resonant E_r field. Since only the field amplitude appears, it corresponds to heating in a dc field. However, since the transit time τ is much shorter than the collision time τ_c, the typical time for diffusion (in velocity space) connected to Joule heating, this term is weighted with τ/τ_c. The exponential factor accounts for the fact that actually a time-varying high-frequency field is considered. The energy gain decreases if the electrons spend a time comparable to the wave period in the resonance region, since they may then be accelerated and afterwards decelerated by the reversing field.

B. Nonlocal kinetic model

The Boltzmann equation written in the form (8) accounts for the plasma inhomogeneity and the steady-state ambipolar electric field. Its solution is obtained here in the approximation of the nonlocal model suggested in [28,29]. The procedure is carried out as described in the recent studies [11,12] on SW sustained discharges based on this model. The limits of applicability of this model require that the characteristic length of *energy* relaxation of the electrons is much larger than the plasma column radius [30]:

$$\lambda_\varepsilon \equiv \lambda_e\sqrt{\frac{\nu_m}{\nu_e}} \gg a. \tag{18}$$

λ_e is the electron mean free path with respect to momentum exchange, ν_e is defined by (7). In this case the total energy [with $\Phi(r)$ the space charge potential]

$$\varepsilon = \frac{mv^2}{2e} - \Phi(r) \tag{19}$$

is approximately conserved during the spatial motion of the electrons so that ε is a meaningful variable. According to Bernstein and Holstein [28] and Tsendin [29] F_0 is then a spatially (almost) homogeneous function of the total energy, where the space dependence can be presented by a small first order correction

$$F_0(\varepsilon, r) = F_0^{(0)}(\varepsilon) + F_0^{(1)}(\varepsilon, r), \tag{20}$$

with $|F_0^{(1)}| \ll |F_0^{(0)}|$. Using this expansion, the solution of the spatially inhomogeneous kinetic equation for F_0 is greatly simplified by spatially averaging via radial integration the kinetic equation over the part of the cross section which is accessible for the electrons with a certain total energy ε. As a result the transport terms cancel out and the following equation is obtained:

$$\frac{d}{d\varepsilon}\left(\bar{D}_\varepsilon\frac{dF_0^{(0)}(\varepsilon)}{d\varepsilon} + \overline{V}_\varepsilon F_0^{(0)}(\varepsilon)\right) = \sum_k\left[\bar{\nu}_k^*(\varepsilon)F_0^{(0)}(\varepsilon) - \bar{\nu}_k^*(\varepsilon+u_k)F_0^{(0)}(\varepsilon+u_k)\right] + \overline{S}_{ee}, \tag{21}$$

with the solid dashes denoting from here on the radial integration mentioned above,

$$\overline{V}_\varepsilon = \frac{2}{a^2}\varkappa\int_0^{r^*(\varepsilon)} u^{\frac{3}{2}}(r)\nu_m(u)r\,dr, \tag{22}$$

$$\bar{\nu}_k^*(\varepsilon) = \frac{2}{a^2}\int_0^{r^k(\varepsilon)}\nu_k(u(r))u^{\frac{1}{2}}(r)\,r\,dr. \tag{23}$$

$\bar{S}_{ee}$ is defined analogously. $r^*(\varepsilon)$ is the turning point radius of electrons traveling in the space charge potential, $r^k(\varepsilon)$ the maximum radius for which the kth inelastic process is possible.

Similarly the spatially averaged energy diffusion coefficient $\overline{D}_\varepsilon$ is given by

$$\overline{D}_\varepsilon = \frac{2}{a^2}\int_0^{r^*(\varepsilon)} D_\varepsilon r\,dr, \tag{24}$$

with

$$D_\varepsilon = D_z + D_r + D_{\text{ql}}. \tag{25}$$

D_z and D_r account for the Joule heating via the axial and radial component of the SW field, respectively, and D_{ql} for the collisionless (quasilinear) heating. Explicitly [with (17)]

$$D_z = \frac{2e}{3m_e} u^{\frac{3}{2}}(r) \frac{|E_z(r)|^2}{2\nu_m(u)} \frac{\nu_m^2(u)}{\nu_m^2(u)+\omega^2}, \tag{26}$$

$$D_r = \frac{2e}{3m_e} u^{\frac{3}{2}}(r) \frac{|E_r(r)|^2}{2\nu_m(u)} \frac{\nu_m^2(u)}{\nu_m^2(u)+\omega^2}, \tag{27}$$

$$D_{\mathrm{ql}} = \frac{\pi e}{2m_e} u^{\frac{3}{2}}(r) \frac{|E_r(r)|^2}{\nu_m(u)} \frac{\tau(u)}{\tau_c(u)} \exp\left(-4\pi\frac{\tau}{T}\right). \tag{28}$$

The spatial averaging procedure used to obtain Eq. (21) relies on the validity of relation (18), which ensures that the spatial motion of electrons is faster than the diffusion in energy space. In this way the whole accessible cross section of the discharge contributes to the formation of the distribution of total energy $F_0^{(0)}(\varepsilon)$. From the solution of Eq. (21) for the distribution function of total energy $F_0^{(0)}(\varepsilon)$, the radially resolved distribution of kinetic energy may be found by backsubstituting: $F_0(u,r) = F_0^{(0)}(\varepsilon = u - \Phi(r))$.

The above approach may be considered a reasonable approximation if pa is not too large (here p is the gas pressure). It has to be stressed that the validity of the nonlocal averaging procedure is principally restricted only by requirement (18) and is valid at arbitrary inhomogeneity of the heating electric field (including the case of plasma resonances). The complete two-dimensional (in u and r) numerical solution [31] of the Boltzmann equation also shows that even in cases of strongly inhomogeneous fields the nonlocal approach remains a good approximation, although the range of applicability is slightly shifted towards lower pressures.

C. Equations completing the closed set

Additional equations are needed to supplement Eq. (21) towards a closed set of equations in order to achieve a self-consistent solution of the problem.

First, the simultaneous determination of the ambipolar potential Φ is obligatory. To this end a fluid approach for ion dynamics can be employed. The continuity and momentum equations for the ions are used. Assuming quasineutrality ($n = n_e = n_i$) and neglecting the ion temperature compared to the electron mean energy one obtains

$$\frac{1}{r}\frac{d(rnv_r)}{dr} = n\nu_i, \tag{29}$$

$$v_r \frac{dv_r}{dr} = -\left[\frac{e}{M_i}\frac{d\Phi}{dr} + (\nu_{in}+\nu_i)v_r\right], \tag{30}$$

where v_r represents the drift velocity of the ions in the ambipolar field, $\nu_i(r)$ is the ionization frequency, and ν_{in} is the ion-neutral collision frequency [32,33]

$$\nu_{in}(v_r) = \nu_{in_0}\left(1 + 0.182\frac{M_i v_r^2}{T_g}\right)^{\frac{1}{2}} \tag{31}$$

due to symmetric charge exchange collisions. ν_{in_0} is the value for small v_r, T_g the gas temperature (in energy units), and M_i is the ion mass. Furthermore, the normalization condition for $F_0^{(0)}$ represents a relation between the plasma density n and the potential $\Phi(r)$:

$$n(\Phi(r)) = n_e(\Phi(r)) = \int_0^\infty F_0(u,r)\sqrt{u}\,du = \int_{-\Phi(r)}^\infty F_0^{(0)}(\varepsilon)\sqrt{\varepsilon+\Phi(r)}\,d\varepsilon. \tag{32}$$

The set of Eqs. (21), (32), (29), and (30) is sufficient to determine simultaneously and self-consistently the unknown quantities $F_0^{(0)}(\varepsilon)$ and thus $F_0^{(0)}(u,r)$, $\Phi(r)$, $n(r)$, and $v_r(r)$. In doing so, the Bohm criterion has to be fulfilled, requiring the drift velocity v_r to be equal to the ion sound speed at the sheath boundary, which is assumed for simplicity to be of zero thickness. This requirement results in the well-known eigenvalue problem for the amplitude of the SW electric field strength.

It may be noted that at higher pressures and electron densities the contribution of ionization from excited atoms may significantly contribute to the ionization frequency $\nu_i(r)$. To account for this effect the solution of the Boltzmann equation has to be coupled to a collisional-radiative model, which describes the different atomic or molecular processes and yields information about the population of excited species. However, in the present study only an approximation of including the stepwise ionization has been performed, by accounting for the most excited state only in a very rough manner. It is assumed that the population of this level is determined by the balance between population from the ground state on the one hand and by losses due to diffusion and ionization on the other hand (see [12]):

$$n_{\mathrm{ex}} = \frac{N n_{e_0}\nu_0}{n_{e_0}\nu_l + D_{\mathrm{ex}}/(a/2.4)^2}. \tag{33}$$

Here N is the ground-state density, ν_0 the frequency for excitation from the ground state, ν_l the loss rate by excitation, D_{ex} the diffusion coefficient of metastables, and n_{e_0} the electron density in the center. The approximation as given by (33) can indicate the direction of changes to be expected due to inclusion of a collisional-radiative model.

Secondly, the electric field profiles and intensities have to be found self-consistently. The field intensities are assumed to vary $\propto \exp[-\int_0^z \gamma(z')dz']\exp(i\omega t)$, with $\gamma(z) = \alpha + i\beta$ giving the local values of wave number and attenuation coefficient at a given position z along the plasma column. With the — radially dependent — electron plasma frequency $\omega_p(r) = [n_e(r)e^2/m_e\varepsilon_0]^{\frac{1}{2}}$ the plasma permittivity is

$$\varepsilon_p(r) = 1 - \frac{\omega_p^2(r)}{\omega(\omega - i\nu_m)}. \tag{34}$$

The field components are then determined by the following equations:

$$\frac{d^2E_z}{dr^2} + \left(\frac{1}{r} + \frac{\gamma^2}{k_n^2(r)}\frac{\frac{d\varepsilon_n(r)}{dr}}{\varepsilon_n(r)}\right)\frac{dE_z}{dr} + k_n^2(r)E_z = 0, \tag{35}$$

$$E_r(r) = -\frac{\gamma}{k_n^2(r)}\frac{dE_z}{dr}. \tag{36}$$

Above the index n stands for plasma, glass, or vacuum, respectively. For k_n the following definition is used ($k_0 = \omega/c$):

$$k_n^2(r) = k_0^2\varepsilon_n(r) + \gamma^2. \tag{37}$$

γ has to be determined so that the continuity of the tangential electric E_z and magnetic H_φ field components is satisfied at the plasma-glass and glass-vacuum boundaries. By this the dispersion relation of the surface waves is given, i.e., the axial wave number β and the damping coefficient α for various $\omega/\overline{\omega_p}$. $\overline{\omega_p}$ is defined as $\sqrt{\overline{\omega_p^2}} \propto \sqrt{\overline{n_e}}$, with $\overline{n_e}$ the electron density averaged over the discharge cross section being a function of z.

Finally, however, the effective damping frequency ν_{eff} introduced [relation (14)] in Sec. II A, where the collisionless energy transfer is described, requires special attention and modifications of Eqs. (35) and (36). The quasilinear term (10) in the Boltzmann equation describes an additional power transfer. On the other hand, the permittivity in Maxwell's equations, i.e., in the field equations (35) and (36), contains only ν_m and thus only the damping due to the Ohmic energy transfer. The sharpness of field resonances would be overestimated without introduction of ν_{eff} also there.

Therefore in the numerical procedure a larger damping frequency, a multiple m_{eff} of ν_m, is introduced which accounts in a heuristic manner for the back reaction of the energy drain from the E_r field via the additional collisionless plasma heating and is actually used for the calculations of the fields:

$$\nu_{\text{eff}} = \nu_m m_{\text{eff}}. \tag{38}$$

With ν_{eff} an effective permittivity ε_{eff} is also introduced, using ν_{eff}, whereas ε_p still designates the use of ν_m only. As a consequence of the above changes, the following field equations [replacing (35) and (36)] are now to be used for the plasma region:

$$\frac{d^2E_z}{dr^2} + \left(\frac{1}{r} + \frac{\gamma^2}{k_0^2\varepsilon_{\text{eff}}(r) + \gamma^2}\,\frac{\frac{d\varepsilon_{\text{eff}}(r)}{dr}}{\varepsilon_{\text{eff}}(r)}\right)\frac{dE_z}{dr}$$

$$+ \left[k_0^2\varepsilon_{\text{eff}}(r) + \gamma^2\right]\frac{\varepsilon_p(r)}{\varepsilon_{\text{eff}}(r)}E_z = 0, \tag{39}$$

$$E_r(r) = \frac{-\gamma}{k_0^2\varepsilon_{\text{eff}}(r) + \gamma^2}\frac{dE_z}{dr}. \tag{40}$$

The values of ν_{eff} are chosen in such a way that consistency between power flux — resulting from Maxwell's equations — and the power absorbed by the plasma — based on the power transfer terms obtained from the Boltzmann equation — is achieved. The idea is to define the effective collision frequency in such a way that the power transfer in the "radial" Ohmic channel and in the collisionless (quasilinear) channel, when calculated with the classical frequency ν_m, is equal to the pure "radial" Ohmic power transfer using ν_{eff}. (Here "radial" means due to the radial electric field.) For both cases the field profile calculation is based on Eqs. (39) and (40) containing ν_{eff}. By this concept the broadening of the field peaks due to the total energy drain from the radial component is accomplished in a consistent way. Concretely the following scheme has been used, where the power transfer via a certain channel (Ohmic via r or z component, collisionless) is characterized by the power absorbed by one electron Θ (for exact definitions see below right at the beginning of the next section).

(1) The field profile is calculated from (39) using a starting guess for ν_{eff}. The sum from the three transfer channels $\Theta_z + \Theta_r + \Theta_{\text{coll-less}}$ is calculated, employing ν_m and the above field profiles.

(2) The same field distributions as in (1) are used. Now the collisionless channel is omitted, Θ_z is calculated using ν_m, but Θ_r is calculated using ν_{eff}.

In order to equalize both sums obtained under (1) and (2), respectively, ν_{eff} has to be adjusted, which requires an iterative procedure. As a starting value of iteration ν_{eff} may be chosen as ν_m times the square root of the initial ratio of $(\Theta_r + \Theta_{\text{coll-less}})/\Theta_r$.

III. RESULTS AND DISCUSSION

A. Mean power absorbed per electron

In order to get an impression of the relative importance of the three heating channels shown in (8) and (21), *the power shares transferred per (average) electron* are calculated: Θ_z and Θ_r for the two Ohmic ones connected to $|E_z|^2$ and $|E_r|^2$, respectively, and for the added *collisionless* one, which results from the *quasilinear* term (10) and is connected with $|E_r|^2$ peaks, here labeled $\Theta_{\text{coll-less}}$.

The terms result from the macroscopic power balance equation. This equation is obtained by multiplying Eq. (21) by the total energy and subsequent integration over the whole energy space. [Note that in Eq. (21) r and ε are independent variables so that the order of integration can be interchanged.] For the three different power transfer channels one obtains

$$\Theta_i = \frac{1}{\overline{n_e}}\int_0^\infty \left[\frac{d}{d\varepsilon}\left(\overline{D}_i\frac{dF_0^{(0)}(\varepsilon)}{d\varepsilon}\right)\right]\varepsilon d\varepsilon, \tag{41}$$

with i designating z, r, ql (coll-less), respectively, and the D_i given by Eqs. (26)–(28). The resultant three Θ terms constitute the energy gain terms in the macroscopic energy balance of the discharge. They are indeed in balance with the collisional loss terms within 1% accuracy, as has been checked as a verification of the numerical method. For the calculation of the Θ terms, of course, the self-consistently calculated $|E_z(r)|^2$- and $|E_r(r)|^2$-field configurations are employed, as described above.

Figure 1 gives an example for Θ_z, Θ_r, $\Theta_{\text{coll-less}}$ and the sum Θ_{total} calculated as outlined as a function of $\omega/\overline{\omega_p}$.

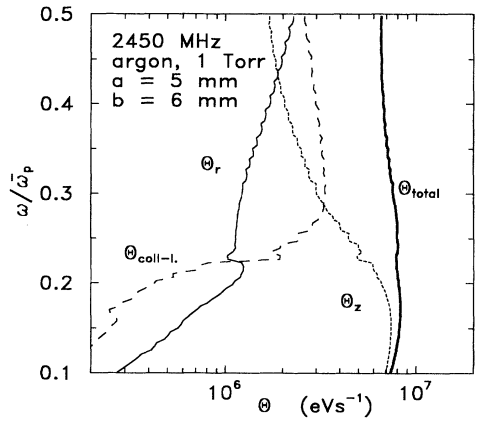

FIG. 1. Power absorbed per average electron Θ_{total}. Θ_z, Θ_r represent Ohmic losses via $|E_z|^2$ and $|E_r|^2$, respectively, $\Theta_{\text{coll-less}}$ collisionless contributions via $|E_r|^2$. $\overline{\omega_p}$ is the plasma frequency of the electron density averaged over the discharge cross section. $\omega/2\pi = 2.45$ GHz, $a = 5$ mm plasma radius, $b = 6$ mm tube radius ($\varepsilon_{\text{glass}} = 4.7$). Gas pressure $p = 1$ Torr argon.

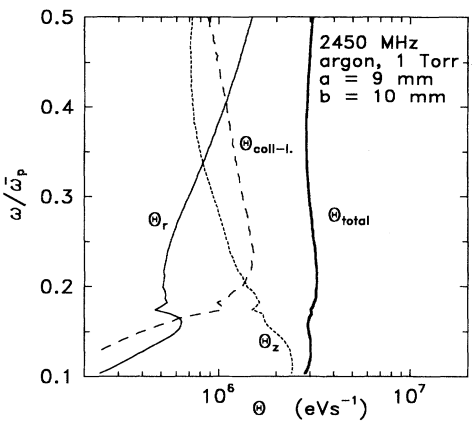

FIG. 3. Conditions are as for Fig. 1, but radius is enlarged to $a = 9$ mm. $p = 1$ Torr argon.

For the parameters considered here ($\omega/2\pi = 2.45$ GHz, $a = 5$ mm, $p = 1$ Torr argon) the Θ_z channel loses its predominance for $\omega/\overline{\omega_p} \approx 0.28$, when $\Theta_{\text{coll-less}}$ becomes larger. It should be mentioned that the Θ_z channel is usually considered as the main (or even the only) power transfer channel over the whole length of the discharge. Thus the predominance of $\Theta_{\text{coll-less}}$ for the higher $\omega/\overline{\omega_p}$ is a remarkable result. It demonstrates that in this regime a totally different physical situation due to the appearance of the plasma resonance is found. However, the variation of Θ_{total} with $\omega/\overline{\omega_p}$ is relatively weak [34]. This "constancy" of Θ_{total} is a consequence of the self-consistency of the problem: Since the ambipolar diffusion losses, which are governed by the ion motion, are (almost) independent of the exact mechanism of energy transfer to the electrons, the ionization frequency has to be independent of this aspect, too. Therefore, in order to maintain a constant ionization, the total power input into the plasma per electron also has to remain constant.

The importance of the results for the power absorbed per electron Θ lies not so much in the sum Θ_{total}, but rather in the distribution to all three channels obtained. Figure 2 gives the result for the conditions of Fig. 1 if a calculation of $\Theta_{\text{coll-less}}$ were omitted: Almost the same values for Θ_{total} are obtained (as has to be expected from the discussion above), its constancy being only slightly less pronounced and Θ_z loses its dominance then at $\omega/\overline{\omega_p} \approx 0.34$ to Θ_r. From diffusion theory it can be expected that the relative radial decrease of the electron density (in relation to the central density) scales with the ratio λ_i/R. Thus the ratio of the central density to the density at the sheath transition n_0/n_s grows with the product of gas pressure times radius, pa. As a consequence of an increased radial density drop, resonance peaks in $|E_r|$ at $\omega_p(r) = \omega$ become possible already at larger averaged (over the cross section) electron densities, i.e., at lower $\omega/\overline{\omega_p}$. Indeed the example of Fig. 3 for the same pressure p as Fig. 1, but for a larger radius ($a = 9$ mm) demonstrates the dominance of $\Theta_{\text{coll-less}}$ to start already at $\omega/\overline{\omega_p} \approx 0.21$, as compared to $\omega/\overline{\omega_p} \approx 0.28$ in Fig. 1. The lowering of pressure

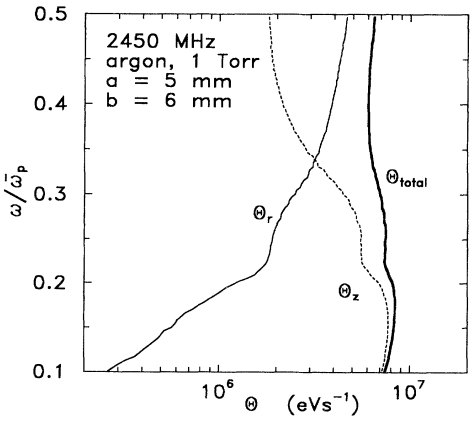

FIG. 2. Conditions are as for Fig. 1, but the calculation assumes absence of the collisionless absorption channel.

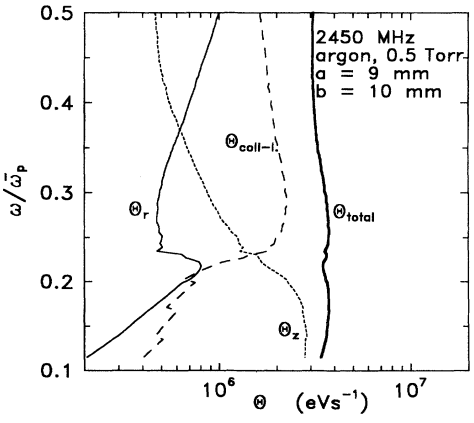

FIG. 4. Conditions are as for Fig. 3, but p is reduced to 0.5 Torr argon.

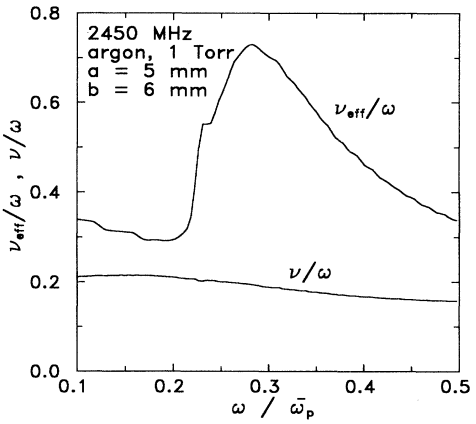

FIG. 5. ν_{eff}/ω and ν_m/ω for conditions of Fig. 1.

to, e.g., 0.5 Torr on the other hand as expected shifts the beginning of dominance of $\Theta_{\text{coll-less}}$ to slightly higher $\omega/\overline{\omega_p}$, as a comparison of Fig. 4 to Fig. 3 shows. Moreover, Fig. 4 demonstrates that with decreasing pressure of course the importance of the Ohmic channels Θ_z and Θ_r is reduced relatively to the collisionless one $\Theta_{\text{coll-less}}$. In Fig. 4 $\Theta_{\text{coll-less}}$ actually remains the largest term up to larger values of $\omega/\overline{\omega_p}$, whereas in Fig. 3 $\Theta_{\text{coll-less}}$ yields the lead to Θ_r at $\omega/\overline{\omega_p} \approx 0.41$, though Θ_z still stays weaker.

The strong role of the collisionless (quasilinear) energy transfer represented by $\Theta_{\text{coll-less}}$ is also reflected in the increase of the effective collision frequency ν_{eff} discussed in Sec. II C exhibiting a pronounced maximum at $\omega/\overline{\omega_p} \approx 0.27$ in Fig. 5 (for the conditions of Fig. 4). The slow ascent of ν_{eff} towards small $\omega/\overline{\omega_p}$ is of less significance, since there $\Theta_{\text{coll-less}}$ competes with Θ_r, but is small compared to Θ_z.

B. Axial density profile

The dependencies of Θ_z, Θ_r, and $\Theta_{\text{coll-less}}$ on $\omega/\overline{\omega_p}$ shown in Figs. 1–4 indicate qualitatively the variation along the discharge axis. For a quantitative transformation from the dependency on $\overline{\omega_p}$ to one on z and in order to study the axial density profile towards the discharge end, the Poynting vector energy transport is considered.

The total power gain per discharge cross section (per unit length) $\Theta_{\text{total}}\pi a^2\overline{n_e}$ has to be covered by the negative divergence of (the real part of) the Poynting vector obtained by integrating over the cross section of the guiding system, with no losses present in vacuum (and glass):

$$-\int_0^\infty \left[\text{div Re}\left(\frac{1}{2}\vec{E}(r)\times\vec{H}^*(r)\right)\right] 2\pi r\,dr = \pi a^2\overline{n_e}\,\Theta_{\text{total}}\,. \quad (42)$$

The derivative $\frac{\partial}{\partial z}$ of the z component of the Poynting vector can be replaced by $\frac{\partial}{\partial\overline{\omega_p}^2}\frac{d\overline{\omega_p}^2}{dz}$:

$$-\pi\,\text{Re}\left\{\frac{d\overline{\omega_p}^2}{dz}\left[\underbrace{\int_0^a \frac{\partial}{\partial\overline{\omega_p}^2}(E_rH^*)r\,dr}_{I_p} + \underbrace{\int_a^\infty \frac{\partial}{\partial\overline{\omega_p}^2}(E_rH^*)r\,dr}_{I_v}\right]\right\} = \pi a^2\overline{n_e}\Theta_{\text{total}}. \quad (43)$$

The contribution by the first integral is expected [16] to be negative and smaller than that of the second one. With I_p and I_v as defined in (43) one finds

$$\frac{d\overline{\omega_p}^2}{dz} = -\frac{a^2\overline{n_e}\Theta_{\text{total}}}{\text{Re}\,\{I_p\}+\text{Re}\,\{I_v\}}\,. \quad (44)$$

The values needed are largely already available from calculation of Θ versus $\omega/\overline{\omega_p}$. For H_φ inside the plasma we can use

$$H_\varphi(r) = \left[-\frac{i\omega\varepsilon_0\varepsilon_{\text{eff}}}{k_0^2\varepsilon_{\text{eff}}+\gamma^2}\frac{\partial E_z}{\partial r}\right]$$

or alternatively

$$H_\varphi(r) = \left[i\frac{\omega\varepsilon_0}{r}\int_0^r r\varepsilon_p E_z\,dr\right]. \quad (45)$$

The axial density profile $\overline{n_e}(z)$ is obtained with $\frac{d\overline{\omega_p}^2}{dz} \propto \frac{d\overline{n_e}(z)}{dz} = f(\overline{n_e})$:

$$z = \int \frac{d\overline{n_e}}{f(\overline{n_e})}\,. \quad (46)$$

For the situation of Fig. 1 the resulting $\frac{d\overline{\omega_p}^2}{dz}$ is given in Fig. 6. In Fig. 7 the related density profile $\overline{n_e}(z)$ starting at $\omega/\overline{\omega_p} = 0.15$ is shown. In Fig. 6 the absolute value of the density slope

$$\left|\frac{d\overline{n_e}}{dz}\right| \propto \left|\frac{d\overline{\omega_p^2}}{dz}\right|$$

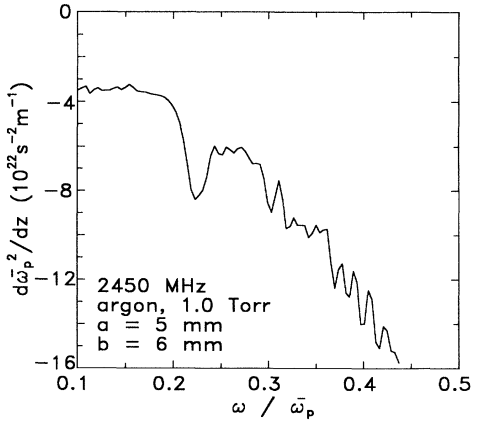

FIG. 6. $d\overline{\omega_p}^2/dz$ for conditions of Fig. 1.

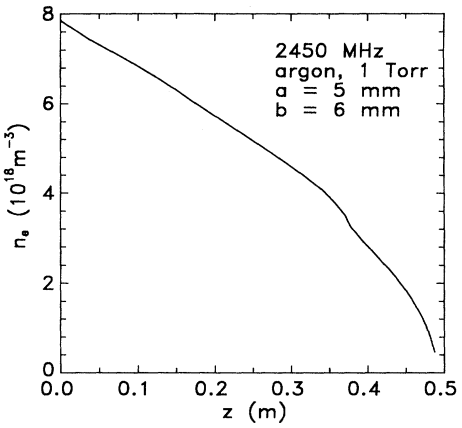

FIG. 7. Integration for $\overline{n_e}(z)$ resulting from Fig. 6, starting at $\omega/\overline{\omega_p} = 0.15$.

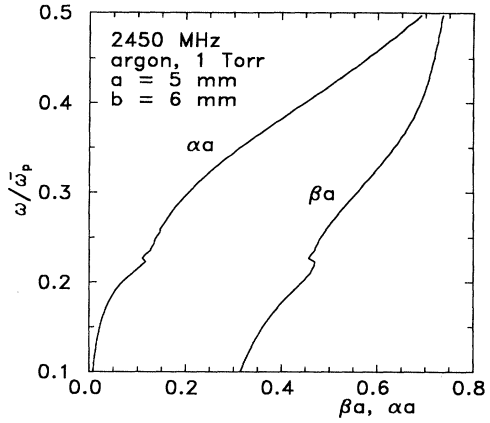

FIG. 8. Axial wave number (β) and damping coefficient (α). Conditions are as for Fig. 1.

increases towards larger $\omega/\overline{\omega_p}$ from a relatively constant value at smaller $\omega/\overline{\omega_p}$. The structure showing in Fig. 6 is only partly significant, much of it stemming from numerical "jitter" which, however, is of little consequence upon the integration of the density profile, as Fig. 7 reveals. Some comparisons to analytical approaches on $\overline{n_e}(z)$ have been given elsewhere [22].

C. Discussion of basic features

The results above are indicative of the important role of plasma resonances in the E_r field and the resultant plasmon excitation. There are some interesting consequences and basic aspects conforming well to analytical expectations given in previous studies [16–24,35].

(1) The excitation of plasma oscillations influences the dispersion of the SWs. Figure 8 (for conditions of Fig. 1) depicts the corresponding real (β) and imaginary (α) parts of the (axial) wave vector. The bends, which appear at $\omega/\overline{\omega_p} \approx 0.23$, can be related to the first appearance of the plasma resonance, which exists for $\omega/\overline{\omega_p} \geq 0.23$. The dispersion modified by interaction with the plasmon mode showing up is of this type, which is to be expected also from analytical consideration: From linear mode interaction with the plasma mode in the low density resonance region basically the type of behavior of β and α as in Fig. 8 can be predicted [35]. In particular, the "bends" can be related to the onset in formation of plasma resonances near the wall of the plasma cylinder. These plasma resonances then move further inwards towards the plasma center with increasing $\omega/\overline{\omega_p}$. These "bends" show up already in numerical solutions of field and dispersion equations for Bessel profiles $n_e(r)$ of different steepness, whenever $\omega_p(r) = \omega$ becomes possible. It should be mentioned that the above "bends" would be more pronounced if the additional broadening of the resonant field peaks by the collisionless heating via ν_{eff} were not included. The "bends" also tend to be stronger and more complicated [35] for lower pressures p and radii a. One example is given in Fig. 9 for the same pressure as in Fig. 8, but with the radius reduced to $a = 3$ mm.

(2) Secondly the additional collisionless heating due to the plasma resonances also exhibits of course an effect on the self-consistent electric field strength, which is necessary to maintain the discharge. This aspect is considered in Fig. 10 for the conditions of Fig. 1. The value of $|E_z|$ at the discharge center is shown, comparing the case including the collisionless power transfer (with $\Theta_{\text{coll-less}}$) to the case excluding this channel. In the former case obviously less field strength is required to maintain the plasma, since the collisionless heating represents an effective source of high energy electrons capable of ionization. Thus only a reduced amount of Ohmic heating is needed to maintain the same total ionization, which in turn results in lower field strengths. This interpretation is also underlined by Fig. 11(a), where the radial distributions of $|E_z|$ and $|E_r|$ are shown for cases both with and without collisionless heating (for the condition $\omega/\overline{\omega_p} = 0.3$). The electric field strengths in the case of collisionless heating included are below those of pure Ohmic heating across the whole radius (and not only in the center). It should be pointed out that the broadening of the $|E_r|$ peak in the

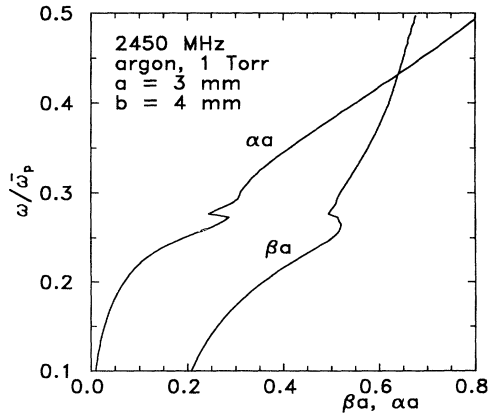

FIG. 9. α and β as in Fig. 8, but the radius is reduced to $a = 3$ mm.

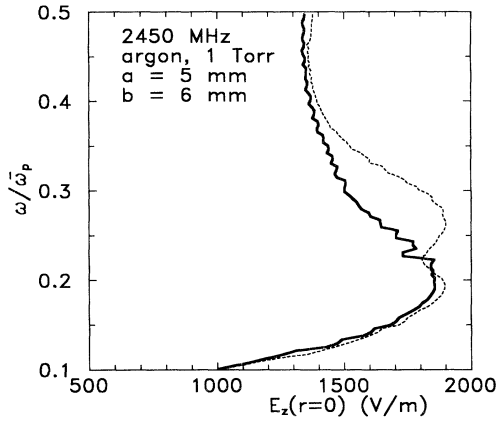

FIG. 10. Maintenance voltage $|E_z|$ at discharge center ($r = 0$) for the conditions of Fig. 1: —. For comparison the values in absence of the collisionless channel are shown (as in Fig. 2): - - -.

presence of collisionless power transfer is due to this additional power drain from the E_r field taken into account via the effective collision frequency ν_{eff}. The appearance of the resonant behavior of $|E_r|$ close to the wall showing up in Fig. 11(a) is also demonstrated in Fig. 11(b) for the same conditions, but with $\omega/\overline{\omega_p}$ increased from 0.3 to 0.4: With decreasing averaged electron density the peak starts to shift away from the wall, the peak height is slightly lowered, and the resonance width is enlarged.

(3) The above interpretation of the collisionless, quasilinear heating to be an efficient mechanism for "hot electron generation" has already been given previously [19] on the basis of an analytical study. Also expression (28) above favors fast electrons. This interpretation is evidenced by the additional bulge of higher energy electrons, in the vicinity of the ionization energy, in the electron-energy distribution function as depicted in Fig. 12 for $\omega/\overline{\omega_p} = 0.25$, the conditions being the same as in Fig. 4. Again cases both with and without collisionless heating are considered. It should be noted that this bulge of hot electrons due to the collisionless heating appears although the electric field strength is considerably lower than in the case without collisionless heating. For the same electric field the hot electron group would be much more pronounced. However, this effect is to some extent masked by the self-consistent determination of the electric field, which requires an (almost) constant total ionization rate and thus distribution functions which are similar in the high energy range.

(4) Finally, the numerical calculations confirm essentially, as is already apparent from Figs. 6 and 7, analytical expectations (for more details see [16–18,22–24]) on the axial density profile $\overline{n_e}(z)$: Though the absorbed power per electron stays largely constant, the changing distribution between the different heating channels — away from the E_z channel — enforces a changed pattern of power flow via the Poynting vector. Resonance peaks in $|E_r|$ that appear result in changed relations between the E-field structure and the density profile $\overline{n_e}(z)$.

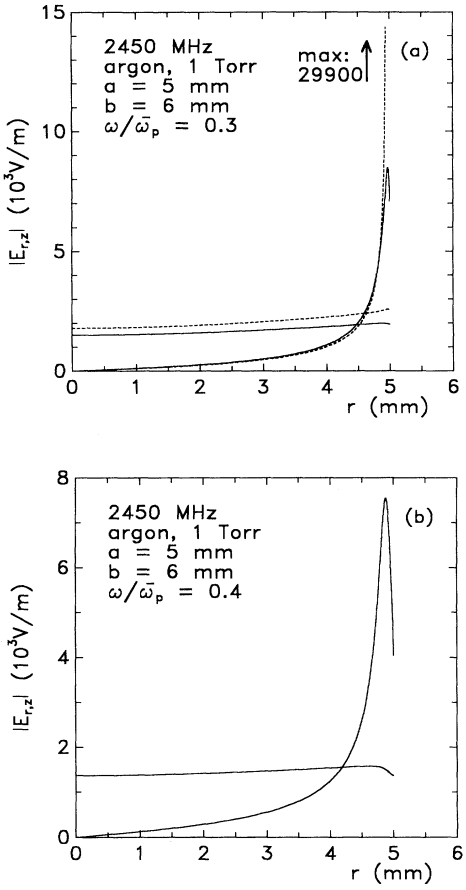

FIG. 11. (a) Maintenance voltages $|E_z|$ and $|E_r|$ as function of radius r for $\omega/\overline{\omega_p} = 0.3$. Otherwise conditions are as in Figs. 1 and 2. As in Fig. 10 calculations are compared with collisionless absorption included (—) and excluded (- - -). The sharply peaked curve represents $|E_r|$. (b) $|E_z|$ and $|E_r|$ as function of radius r for $\omega/\overline{\omega_p} = 0.4$. Otherwise conditions are those of Figs. 1, 2, and (a).

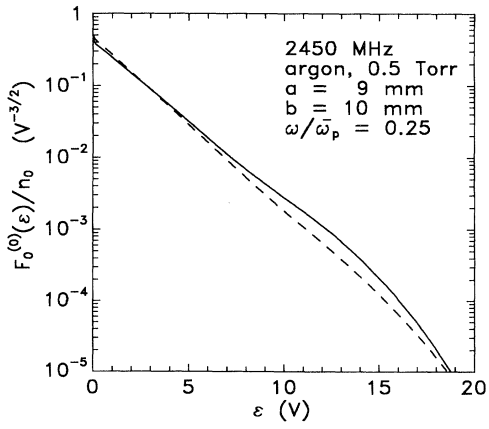

FIG. 12. Electron-energy distribution function F_0, normalized to the electron density n_0 at the center of the discharge, for the conditions of Fig. 4, with $\omega/\overline{\omega_p} = 0.25$. The two situations with collisionless absorption included (—) and excluded (- - -) are compared.

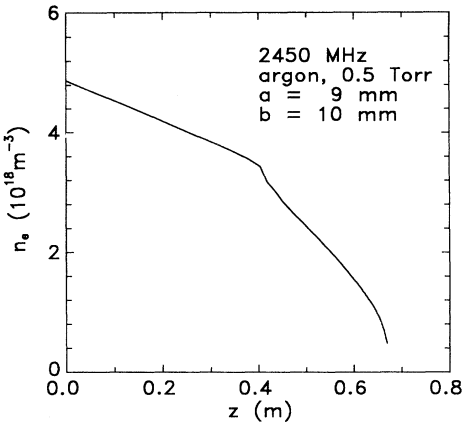

FIG. 13. Axial density profile $\overline{n_e}(z)$ as in Fig. 7, but the conditions are changed to $a = 9$ mm and $p = 0.5$ Torr, starting at $\omega/\overline{\omega_p} = 0.19$.

As a consequence considerable deviations from the usual linear profile $\overline{n_e}(z)$ [16,17] appear towards discharge sections further away from the wave launcher, where $\overline{n_e}(z)$ decreases faster than linearly. Indeed this behavior has been predicted already on the basis of analytical estimates [22–24]. The density profile $\overline{n_e}(z)$ is expected to terminate its linear behavior at some position $z \approx z_1$ and thus to approach a square root dependence of the form $\overline{n_e}(z) \propto \sqrt{1 - \text{const} \times (z - z_1)}$. This behavior is obvious in Fig. 7 and also in Fig. 13, which gives an additional example addressing a situation at larger radius and smaller pressure than in Fig. 7. By comparison of both figures it can again be seen that plasma resonance effects are more important for lower pressures and larger discharge tubes. In Fig. 13 the deviation from a linear $\overline{n_e}(z)$ starts at about $\omega/\overline{\omega_p} = 0.22$. The detailed structure is influenced by the changes of the resonance conditions when the resonance moves radially inward with increasing $\omega/\overline{\omega_p}$ (decreasing $\overline{n_e}$), e.g., the changing resonance peak width Δ.

IV. CONCLUSIONS AND OUTLOOK

In the present investigation the existence of the resonance of the radial SW electric field component has been discussed on the basis of a self-consistent kinetic model of the SW discharge. Thus in contrast to previous analytical studies it was not necessary to postulate the existence of the resonance or to make assumptions about the suitable radial density profiles. Moreover the existence of parameter ranges with a *dominance* of plasmon influence in SW sustained plasmas is demonstrated.

The numerical calculations confirm and extend previous analytical considerations [16–24,35] in many details, in particular concerning the role of plasmon mode excitation [19–24].

The total absorbed power averaged per electron, Θ_{total}, remains more or less constant, although the single contributions change drastically. This is exactly the behavior which has to be expected, since for the maintenance of the plasma it should be unimportant by which channel the energy is delivered.

In general the following conclusions on the importance of the collisionless heating can be drawn from a number of calculations.

(1) The collisionless heating via the resonant E_r field is important in the microwave regime, since here low ν_c/ω ratios can be achieved at simultaneously high pressures. The low ν_c/ω assures a pronounced resonance of the E_r-field component.

(2) The collisionless heating is important for a larger axial part of the discharge vessel for large radii and high pressures, since both quantities affect the λ_i/a ratio, which determines the electron density at the plasma sheath boundary: For larger radii the range of predominant collisionless heating extends to higher electron densities, i.e., to lower $\omega/\overline{\omega_p}$. The same holds true for increasing pressure, even though the relative strength of Joule heating increases with pressure. On the other hand, the relative strength of collisionless heating is, of course, larger for lower pressures.

The accuracy of the nonlocal kinetic model used is, of course, limited: Its applicability is obviously best for not too high values of pa [12]. Otherwise the solution of the complete two-dimensional (in u, r) kinetic equation for the isotropic part of the distribution function is required, which is beyond the scope of the present paper. The alternative of using a "local" model, employing the spatially homogeneous Boltzmann equation for distributions locally in equilibrium with the electric field, is of little interest when resonance features connected to plasmon interaction are addressed, since it requires higher pressure p, the collisional damping being then too large. Further applications of the nonlocal approach as well as complete two-dimensional treatments in cases of rather inhomogeneous radial electric field distributions are desirable. In this context it may be mentioned that the nonlocal approach has already successfully been applied to the modeling of other types of high-frequency discharges which are characterized by strongly inhomogeneous fields too, such as the capacity coupled rf discharge [36,37] and the inductively coupled rf discharge [38,39].

The overall accuracy of the absolute values of Θ presented should not be overestimated, but is expected to stay within about a factor 2. Ways of improvement are largely obvious, e.g., by more accurate future two-dimensional calculations and inclusion of more processes (involving also more complete collisional-radiative excitation-ionization models). Also dropping the used simplification of a radially constant collision frequency ν_m would be more accurate with a view to radially varying distribution functions. Preliminary results on this latter aspect have shown no drastic influence. In this article, however, the relative importance of various power input channels is expected to be described reasonably accurately, since basically a self-consistent approach is used in the calculations in particular concerning the formation of the radial density profiles. The range of impact for plasmon interaction seems to be pointed out reliably.

The present model implies the validity of the zero order geometrical optics approach concerning axial variations,

since with respect to z local dispersion relations are used. Though the axial density changes are rather slow (with a scale length large compared to the radius), towards the very end of the discharge the situation may become more difficult due to two-dimensional features. In particular, in cases as additional phenomenon the electrostatic "system" resonances may have to be considered [5,40], including also additional loss processes encountered then (but neglected here), e.g., heat conduction and diffusion end losses. Some relevant aspects are to be considered elsewhere.

If the usual scaling of Θ_{total} is assumed, the calculated values are consistent with — though slightly larger than — the values given for 2.45 GHz in [41] for rather high $\overline{\omega_p}$ at small a. Extension of the numerical calculations as performed above to lower $\omega/\overline{\omega_p} < 0.1$ seem to indicate some decrease of Θ_{total}, but the accuracy of the numerical procedure in that range remains yet to be improved. For future work comparisons with measurements are desirable under conditions similar to those addressed here. From preliminary measurements of the electric field intensity inside the plasma by probe-antennas there are first experimental hints on the existence of the plasma resonance [42].

Finally it should be stressed that in future situations at much lower wave frequency ω must be considered in modeling and experiment. There the role of plasmon interaction may be different. At low ω and low p plasmon effects may be less important and other effects must be accounted for, such as potential electrostatic resonances [5,40].

ACKNOWLEDGMENTS

The authors are indebted to Deutsche Forschungsgemeinschaft for support through SFB 191 and exchange programs. Support by the EC (Contract No. CT93101) is also gratefully acknowledged.

[1] *Microwave Excited Plasmas*, edited by M. Moisan and J. Pelletier (Elsevier, Amsterdam, 1992).
[2] *Microwave Discharges: Fundamentals and Applications*, Vol. 302 of *NATO Advanced Study Institute, Series B: Physics*, edited by C.M. Ferreira and M. Moisan (Plenum, New York, 1993).
[3] K.N. Stepanov, Zh. Tekh. Fiz. **35**, 1002 (1965) [Sov. Phys. Tech. Phys. **10**, 773 (1970)].
[4] M. Zethoff and U. Kortshagen, J. Phys. D **25**, 1574 (1992).
[5] Yu.M. Aliev, J. Berndt, H. Schlüter, and A. Shivarova, J. Electromagn. Waves Appl. (to be published).
[6] C.M. Ferreira, J. Phys. D. **14**, 1811 (1981).
[7] C.M. Ferreira and M. Moisan, Phys. Scr. **38**, 382 (1988).
[8] U. Kortshagen, H. Schlüter, and A. Shivarova, J. Appl. Phys. **24**, 1571 (1991).
[9] U. Kortshagen and H. Schlüter, J. Phys. D **25**, 644 (1992).
[10] A.B. Sá, C.M. Ferreira, S. Pasquiers, C. Boisse-Laporte, P. Leprince, and J. Marec, J. Appl. Phys. **70**, 4147 (1991).
[11] U. Kortshagen, J. Phys. D **26**, 1691 (1993).
[12] U. Kortshagen, Phys. Rev. E **49**, 4369 (1994).
[13] U. Kortshagen, A. Shivarova, E. Tatarova, and D. Zamfirov, J. Phys. D. **27**, 301 (1993).
[14] V.M.M. Glaude, M. Moisan, R. Pantel, P. Leprince, and J. Marec, J. Appl. Phys. **51**, 5693 (1980).
[15] I. Zhelyazkov, E. Benova, and V. Atannassov, J. Appl. Phys. **59**, 1466 (1986).
[16] Yu.M. Aliev, K.M. Ivanova, M. Moisan, and A. Shivarova, Plasma Sources Sci. Technol. **2**, 145 (1993).
[17] Yu.M. Aliev, I. Ghanashev, H. Schlüter, A. Shivarova, and M. Zethoff, Plasma Sources Sci. Technol. **3**, 126 (1994).
[18] Yu.M. Aliev, A.V. Maximov, H. Schlüter, and A. Shivarova, IEEE Trans. Plasma Sci. (to be published).
[19] Yu.M. Aliev, V.Yu. Bychenkov, A.V. Maximov, and H. Schlüter, Plasma Sources Sci. Technol. **1**, 126 (1992).
[20] Yu.M. Aliev, in *Microwave Discharges: Fundamentals and Applications*, Vol. 302 of *NATO Advanced Study Institute, Series B: Physics*, edited by C.M. Ferreira and M. Moisan (Plenum, New York, 1993), p. 105.
[21] Yu.M. Aliev, A.V. Maximov, and H. Schlüter, Phys. Scr. **48**, 464 (1993).
[22] Yu.M. Aliev, S. Grosse, A.V. Maximov, H. Schlüter, and A. Shivarova, in *Europhysics Conference Abstracts*, edited by C. M. C. van de Sanden (European Physical Society, Geneva, 1994), Vol. 18E, p. 199.
[23] Yu.M. Aliev, A.V. Maximov, H. Schlüter, and A. Shivarova, Phys. Scr. **51**, 257 (1995).
[24] Yu.M. Aliev, A.V. Maximov, H. Schlüter, and A. Shivarova, J. Plasma Phys. **52**, 321 (1994).
[25] A.A. Vedenov, E.P. Velikov, and R.Z. Sagdeev, Nucl. Fusion **1**, 82 (1961).
[26] I.P. Shkarofsky, T.W. Johnston, and M.P. Bachynski, *The Particle Kinetics of Plasmas* (Addison-Wesley, Reading, MA, 1966).
[27] V.E. Golant, A.P. Zhilinsky, and I.E. Sakharov, *Fundamentals of Plasma Physics* (Wiley, New York, 1980).
[28] I.B. Bernstein and T. Holstein, Phys. Rev. **94**, 1475 (1954).
[29] L.D. Tsendin, Zh. Eksp. Teor. Fiz. **66**, 1638 (1974) [Sov. Phys. JETP **39**, 805 (1974)].
[30] A.V. Timofeev, Zh. Tekh. Fiz. **40**, 192 (1970) [Sov. Phys. Tech. Phys. **15**, 140 (1970)].
[31] C. Busch and U. Kortshagen, Phys. Rev. E **51**, 280 (1995).
[32] S.C. Brown, *Basic Data of Plasma Physics* (Wiley, New York, 1959).
[33] V. Martisovits, J. Phys. B. **3**, 850 (1970).
[34] Yu.M. Aliev, A.V. Maximov, H. Schlüter, U. Kortshagen, and A. Shivarova (unpublished).
[35] Yu.M. Aliev, U. Kortshagen, M. Maximov, A. Shivarova, and S. Grosse (unpublished).
[36] I.D. Kaganovich and L. Tsendin, IEEE Trans. Plasma Sci. **20**, 66 (1992).
[37] S.V. Berezhnoi, I.D. Kaganovich, E.L. Levin, and L.D. Tsendin (unpublished).

[38] U. Kortshagen, I. Pukropski, and M. Zethoff, J. Appl. Phys. **76**, 2048 (1994).
[39] U. Kortshagen and L.D. Tsendin, Appl. Phys. Lett. **65**, 1355 (1994).
[40] Yu.M. Aliev, J. Berndt, H. Schlüter, and A. Shivarova, Plasma Phys. Control. Fusion **36**, 937 (1994).
[41] P.A. Sá, J. Loureiro, and C.M. Ferreira, J. Phys. D. **25**, 960 (1992).
[42] H. Schlüter, in *Microwave Plasma and Its Application*, edited by Yu.A. Lebodev (Moscow Physical Society, Moscow, 1995), p. 366.